International Journal of Mechatronics and Manufacturing Systems

ISSN online: 1753-1047 - ISSN print: 1753-1039
https://www.inderscience.com/ijmms

Hybrid finite elements method-artificial neural network approach for hardness prediction of AA6082 friction stir welded joints

Mariangela Quarto, Sara Bocchi, Gianluca D'Urso, Claudio Giardini

DOI: 10.1504/IJMMS.2022.10048834

Article History:

Received:	29 September 2021
Last revised:	27 June 2022
Accepted:	12 January 2022
Published online:	16 August 2022

Hybrid finite elements method-artificial neural network approach for hardness prediction of AA6082 friction stir welded joints

Mariangela Quarto, Sara Bocchi, Gianluca D'Urso* and Claudio Giardini

Department of Management, Information and Production Engineering, University of Bergamo,
Via Pasubio7/b, 24044, Dalmine (Bergamo) – Italy
Email: mariangela.quarto@unibg.it
Email: sara.bocchi@unibg.it
Email: gianluca.d-urso@unibg.it
Email: claudio.giardini@unibg.it
*Corresponding author

Abstract: One of the main important aspect of friction stir welded parts is the different hardness values reached in the characteristic welding zone, as a function of the maximum temperature derived from the welding process. Indeed, these differences affect the mechanical properties and the service quality of component. For these reasons, a hybrid model for predicting the final hardness of the single points of the welding as a function of the maximum reached temperature is developed. Specifically, the hybrid approach takes into account the finite element method (FEM) and the artificial neural network (ANN). The FEM model was set-up and the temperature map output was introduced into the ANN together with experimental results for the ANN training. The hybrid approach FEM-ANN provides a robust framework for forecasting aluminium hardness after the FSW process without experimentally investigating each welding.

Keywords: hybrid approach; FEM; finite element analysis; neural network; process sustainability; FSW; friction stir welding; aluminium alloy; artificial intelligence; forecasting model; hardness prediction.

Reference to this paper should be made as follows: Quarto, M., Bocchi, S., D'Urso, G. and Giardini, C. (2022) 'Hybrid finite elements method-artificial neural network approach for hardness prediction of AA6082 friction stir welded joints', *Int. J. Mechatronics and Manufacturing Systems*, Vol. 15, Nos. 2/3, pp.149–166.

Biographical notes: Mariangela Quarto is a researcher of the Department of Management, Information and Production Engineering, University of Bergamo. She received her PhD in Economic and Management of Technology from University of Pavia. Her research interests include micro-EDM, optimisation processes from economical and technical point of view through the application of models and algorithms and additive manufacturing processes.

Sara Bocchi is a research fellow of the Department of Management, Information and Production Engineering, University of Bergamo. She received her PhD in Technology Innovation and Management at the University of Bergamo. Her research interests include friction Stir Welding and Friction Stir Extrusion process and modelling through the application of finite element

simulation, with particular focus on their optimization and the efficiency of the joints both from the mechanical characteristics and corrosion behaviour point of view.

Gianluca D'Urso is a Full Professor and Deputy Director of the Department of Management, Information and Production Engineering, University of Bergamo. He is Director of the first level executive Master in "Smart Manufacturing Management e Digital Transformation". His research interests include forming technologies, friction stir welding, micro-manufacturing with a particular focus on micro-EDM process, discrete event and finite element simulation and during last year also additive manufacturing processes.

Claudio Giardini is a Full Professor of the Department of Management, Information and Production Engineering, University of Bergamo. His research interests include the plastic deformation of metal, optimisation of cutting operations, micro-EDM, application of quality tools in manufacturing processes.

1 Introduction

Nowadays, one of the most important challenges is the sustainable development to reduce global pollution. This challenge especially regards CO_2 direct and indirect emissions, an issue strictly related to the industry field which contributes about 40% of the world emissions; in fact, CO_2 emissions due to the industry have increased in recent years, except for the recent COVID-19 effect. Within the production field, manufacturing is one of the most polluting sectors (IEA, 2020). Among the manufacturing processes, friction stir welding (FSW) is proving to be a promising green technology as it is characterised by high energy efficiency, due to the involved lower temperatures with respect to the traditional fusion welding techniques, and respect for the environment, because of the limited waste material and the avoided radiation and hazardous fumes (Shrivastava et al., 2015; Bevilacqua et al., 2017; Sethi et al., 2021).

FSW technology is a solid-state welding process (the temperature reached during processing always remains below the solidus temperature of processed material, i.e., approximately 660°C for aluminium) which allows to permanently join materials that are difficult to be welded with traditional techniques.

The joining of the parts is achieved by a suitable tool which has the task of mixing the material along with the flaps in the plastic field generating dynamic recrystallisation phenomena.

This innovative technology allows staying below the melting point of the material limiting metallurgical defects related to the solidification process, such as hot cracks, gaseous inclusions and slags in the molten area. Furthermore, the processed material undergoes intense plastic deformation, generating a microstructure consisting of recrystallised small and equiaxed grains which guarantee a minor deterioration of mechanical properties compared to fusion welds. Since FSW process allows to weld rather thick pieces in a single pass, it is quite easy to apply it in a high rate production system.

FSW provides joints welded without overlapping flaps and connecting parts ensuring the welding of dissimilar materials, with a reduction in both weight and cost, (Mishra and

Ma, 2005). Although the heat generated by the friction between the pieces to be welded and the tool is much lower than that developed by a traditional welding technique, the reached temperatures are high enough to cause the problem of softening in welded joints, which is even more pronounced in precipitation hardening aluminium alloys. The softening is due to the dissolution and subsequent enlargement of the hardening precipitates with consequent reduction of the mechanical properties of the joints. For these reasons, the reduction of heat input is very important for significantly reducing the softening of the joint, thus improving the mechanical properties of the weld, including the hardness (Fonda and Bingert, 2004). This can be gained considering the effect of the welding parameters or considering an external cooling.

Regarding the process parameters, the relationship between the welding speeds (feed rate and rotational speed) and the heat input provided during the process is very complex but, in general, increasing the rotational speed and reducing the feed rate, generate a higher temperature welding (Ren et al., 2007).

Lee et al. (2004) described higher hardness values recorded on FSWed AA6061 for high tool rotational speed. The authors correlated this behaviour to the presence of many second phase precipitation hardeners (Lee et al., 2004). With regards to the external cooling, recent works (Heirani et al., 2017; Wahid et al., 2018) introduced the Underwater Friction Stir Welding technology (UFSW): water is used as a liquid coolant to control temperature profiles and reduce heat absorbed by the welded joints. The water high heat absorption capacity allows the heat removal from the heat-affected zone (HAZ) and thermo-mechanically affected zone (TMAZ). The water-cooling effect prevents from reaching the solubilisation temperature of the hardening precipitates, avoids the coarsening of the grains, and allows to increase the mechanical resistance of the welded joints (Wahid et al., 2018). Better in-process control of the microstructure of the welded joints would limit the need for post-weld heat treatments. The heat input and the peak temperature are fundamental parameters for the control of the microstructure and mechanical characteristics of the welded joints. Zhao et al. (2014) showed that the presence of water cooling ensures a clear reduction in temperature, measured with thermocouples inserted in the section of the joints to be welded, with respect to the same system without the water cooling. The water-cooling effect is also evident for the micro-hardness values measured for different joints on different aluminium alloys. For heat-treatable alloys, it was noticed that, generally, the zone of minimum hardness is found in correspondence with the HAZ or TMAZ in the advancing side for FSW. Conversely, for UFSW welded joints, the area of minimum hardness is translated towards the nugget both in advancing and retreating side and the softening region is more contained, guaranteeing an increment in hardness values (Fonda and Bingert, 2004; Rui-Dong et al., 2011; Zhao et al., 2014; Qingzhao et al., 2015).

Despite these characteristics, the UFSW also has some weaknesses. Wahid et al. (2018) demonstrated that the mechanical behaviour of the UFSWed are affected by the voids owing to the presence of some particles of water trapped in the joint and their evaporation for the temperatures subsequently reached during the process.

Since FSW is a quite recent process, the development of models and simulation techniques is useful for better understanding its physics (Chen et al., 2003; Assidi et al., 2010; He et al., 2014). In the last decade, some models for the simulation of the FSW process, based on different formulations and approaches, were implemented on some well-known commercial codes. Zhang and Zhang, (2008) set up a model using the commercial code ABAQUS and an Arbitrary Lagrangian-Eulerian (ALE) formulation

with adaptive mesh. Chen and Kovacevic (2003) used the commercial finite element package ANSYS to simulate the entire welding process considering the thermal impact and the evolution of the stresses in the weld by in view of the mechanical effect of the tool. Chao et al. (2003) studied a steady-state heat transfer model for the tool efficiency with a FEA Code ABAQUS. The model evidenced the high heat efficiency of the FSW process demonstrating that only about 5% of the heat generated by the friction process flows to the tool and the rest flows to the workpiece. Colegrove et al. (2007) created in FLUENT a numerical model for predicting the heat generation in FSW, fixing the material and process characteristics in aerospace AA2024, AA6013 and AA7449 (e.g., hot deformation and thermal properties, process parameters, tool and plate dimensions). However, the application of the various FEM models does not allow an immediate analysis of the mechanical characteristics of the simulated pieces, except for the stresses generated by the process itself. To fill this gap, it is possible to resort to other types of predictive tools, among which the artificial neural network (ANN) algorithm has stood out in recent years. Many researchers have recently developed ANN models to predict the effect of different welding parameters and different process conditions, especially on mechanical and metallurgical properties of FSWed joints. The relation between the feed rate and rotational speed with the ultimate tensile strength of FSWed AA7075 joints was studied by Sönmez et al. (2017) developing an ANN model. Dehabadi et al. (2016) applied an ANN to predict Vickers micro-hardness of FSWed AA6061 sheets, founding a good correlation between the predicted and experimental results.

Despite the growing interest in these predictive algorithms, from the literature review, it seems that the ANN method applied to the FSW process was primarily focused on the identification of a specific link between the process parameters and the output mechanical behaviour.

In the present paper, a hybrid approach involving FEM and an ANN was developed for predicting the hardness of joint obtained after the FSW process. In this case, the term hybrid is related to the idea of applying different approaches for the same purpose; in particular, the output of the first part of the model can be used as input for the second part. According to the literature review, a mixed ANN and FEM approach has never been applied to study the behaviour of the welded material after the FSW process. This approach provides a finite element model for the simulation of a FSW process to predict the temperature distribution using both air and water-cooling systems. To create a robust model, a sensitivity analysis was conducted to study the relationship between the input and the output variables. The validation process of the FEM model was performed through a comparison with experimental data, assuming as a reference case a previous work by Bocchi et al. (2021). Several welding operations were carried out by measuring the reached temperatures by means of thermocouples and an infrared camera. The simulative and experimental results were compared showing a satisfactory matching. The temperature data extrapolated by the simulations post-processing analyses were used as input for the ANN to predict the hardness values characterising a specific position on the surface of the samples.

The developed hybrid approach allows predicting one of the most critical aspect of the welded product, since the increment of temperature during the process can generate a modification in the microstructure and then in the characteristics of the final product. This kind of approach could be useful in the production field as it is able to predict precise and well-determined in space hardness values only as a function of the temperatures locally reached during the welding process.

2 Proposed hybrid FEM-ANN approach

The proposed FEM-ANN approach is sketched in Figure 1. Once the model has reached a satisfactory level of accuracy and robustness, the simulated results were used to generate the dataset used for the ANN training step. The numerical simulation already represents a suitable tool for forecasting process results, but its integration with the neural network can result in an improvement of a prediction model.

Figure 1 Hybrid FEM-ANN approach flowchart (see online version for colours)

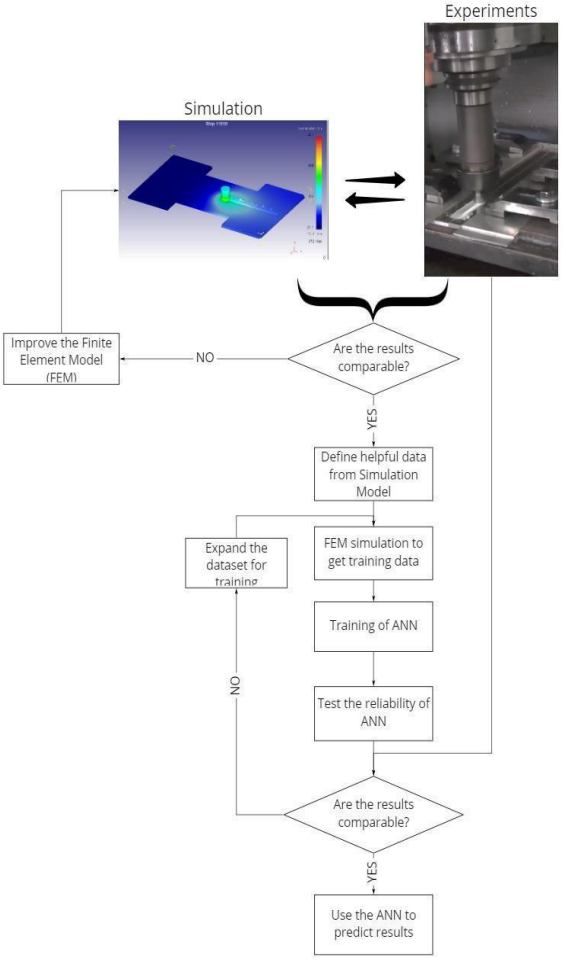

3 FSW simulation model setup

A 3D FEM Lagrangian model was set up using the commercial software DEFORM 3D^{TM}. The tool was modelled as a rigid object using AISI-1045 steel as reference material (defined between 20°C and 1100°C). The plates to be welded were modelled as a single plastic workpiece made of Aluminium-6061 (defined between 250°C and

480°C). Both aluminium and steel with their material flow stress data were chosen among those available in the Deform library database (with their related material constitutive and physical properties).

The assumption to consider the tool as a rigid object and the workpiece as plastic is reasonable because of the significantly lower yield strength of the aluminium with respect to the yield strength of the steel tool. Finally, the workpiece was discretised using 100,000 tetrahedral elements, as shown in Figure 2.

Figure 2 Mesh of the aluminium workpiece (see online version for colours)

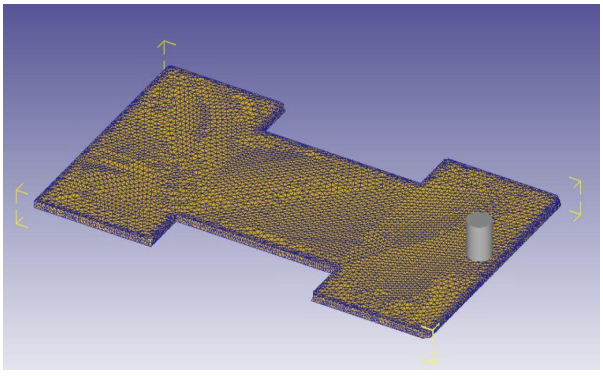

In order to better simulate the entire FSW process, it was divided into three main steps. In the first one, the tool, which is not yet in contact with the workpiece, starts to rotate and translate in the vertical direction until the tool shoulder is completely in contact with the aluminium workpiece. In the second phase, the advancing stage, the tool advances along the welding line, until the entire length of the sheet has been involved in the process. The last step involves the ascent and the detachment of the tool from the workpiece. For the whole process, the rotational speed and the feed rate were set equal to 2400 rpm and 375 mm/min respectively, which are the optimal welding parameters obtained from a previous work (Bocchi et al., 2019).

Regarding the thermal part of the simulation, the heat exchange with the environment was kept constant. Specifically, the heat exchange with the environment was set equal to 0.02 N/(mm·s·°C) for the air-cooled FSWed joints; while three levels were tested (0.3, 0.4, 0.6 N/(mm·s·°C)) for the water-cooling condition for obtaining the better match with the experimental results. The heat exchange with the environment for the water-cooling condition was maintained constant only within a local window moving with the tool only during the advancing stage, once the best coefficient has been identified. This choice was made to get closer to the experimental campaign, where the flux of water hit only the already welded part of the joint. Into the local window, the water temperature was maintained constant at 20°C.

During the last stage of the process, the mentioned local window remains in the reached position at the end of the welding advancing step, until the entire simulation process stops. This choice was made to obtain a model as close as possible to the experimental conditions. A sensitivity analysis, involving the parameters reported in Table 1, was carried out following an inverse characterisation method based on previously collected experimental data reported in prior research papers (Bocchi et al., 2019, Bocchi et al., 2021).

Table 1 Parameters and their range considered for the sensitivity analysis

Parameters	*Value*	
	Min	*Max*
Friction coefficient aluminium-tool	0.4	1
Thermal conductivity	100 N/(mm·s·°C)	600 N/(mm·s·°C)
Aluminium emissivity	0.2	1
Heat transfer coefficient aluminium-tool	11 N/(mm·s·°C)	10000 N/(mm·s·°C)

3.1 FEM model validation

The simulated results were compared with the experimental data for validating the FEM model. The experimental campaign was performed using a CNC machine tool. Butt joints were carried out on AA6082-T6 sheets having a thickness equal to 4 mm. A tapered cylindrical tool (pin minimum and maximum diameters equal to 4 mm and 6 mm, pin height equal to 3.9 mm) and flat shoulder (diameter equal to 16 mm) was considered. The adopted values of tool rotation speed and feed rate are the same applied in the simulations (Bocchi et al., 2019).

Two cooling conditions were taken into account:

1 traditional, with air

2 room-temperature water, insulating the area still to be welded through a bulkhead mounted on the spindle.

In order to quantitatively measure the temperature variation reached in the joint with and without the water-cooling system, three type K thermocouples were positioned in the cross-section of the plates at different depths to be able to detect the temperature at the three fundamental zones of the welding: 10 mm from the nugget (nugget proximity), TMAZ and HAZ. Thermocouples positions are represented in Figure 3. It was chosen to place the thermocouples in the advancing side because, although the process is almost symmetrical in terms of achieved hardness and mechanical properties, this part has proved to be hotter than the retreating side, as demonstrated by Sorger et al. (2017). A Flir System ThermoVision A40 infrared camera was used in order to measure the peak temperature reached by the nugget, where the remixing of the material prevents the contact measurement.

The combinations of parameters used in the FEM simulations are shown in Tables 2 and 3. The columns relating to the outputs show the percentage differences with respect to the reference temperatures experimentally measured by the thermocouples in the reference area (nugget proximity, TMAZ and HAZ). In the cited tables, the friction coefficient between aluminium and tool is indicated by A, the thermal conductivity of aluminium by B, the aluminium emissivity by C and the heat transfer coefficient between aluminium and tool by D. Regarding the friction model considered for the FE simulations, a constant shear friction factor m was used for the tool–sheet interface.

The main difference between the two models is represented by the presence of a fifth parameter for the water-cooled process, the heat exchange with the environment, represented in Table 3 by the letter E. The optimal combinations able to better reproduce the process behaviour and the temperature distribution are highlighted in Table 2 for

air-cooled joints and in Table 3 for water-cooled welds, as results from the several simulations conducted.

Figure 3 Thermocouples housings inside the plates to be welded (Bocchi et al., 2021). The C-shape of the advancing side was due to the need for the right housing of the thermocouples, while the I-shape was related to the symmetry of the welded plate (see online version for colours)

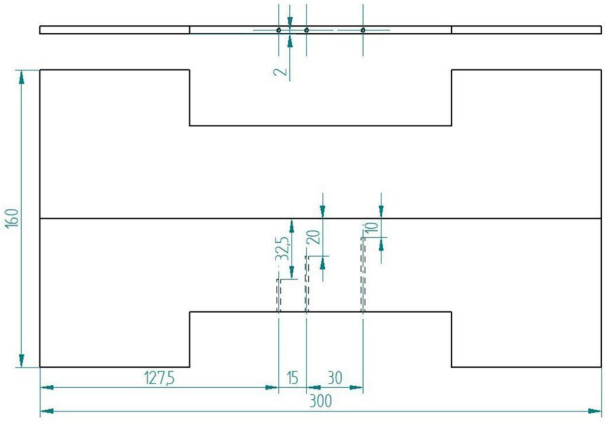

The validation of the model was performed comparing the temperature values predicted (registered in the corresponding positions) and the maximum temperatures experimentally measured by the thermocouples. Figures 4 and 5 show the accuracy level of the forecasted temperature. In particular, an acceptable deviation from the experimental values can be observed; in fact, as reported by Arora et al. and by Zhu et al., the simulated values are considered in close agreement with the experimental ones, and thus trustable for the further phases of the analysis, if the forecasting error value is around 15% (Zhu and Chao, 2004; Arora et al., 2012).

From the graphs shown in Figures 4 and 5, it is possible to state that one of the main strengths of the simulation model is the possibility to predict very accurately the reached maximum temperatures in both air-cooled and water-cooled conditions.

Regarding the cooling thermal gradient, its prediction proved to be less accurate in the case of air-cooled welds due to the simplifying assumptions applied to the model. Specifically, the cooling thermal gradient is considered as the time required to decrease the sheet temperature to 50°C. This is demonstrated in the graphs by showing the time necessary for the drop of the temperature from the peak temperature to 50°C. This different temperature trend in the air-cooling phase (Figure 4) is probably due to the presence of the support plate on which the sheets to be welded are strongly constrained during the experimental campaign.

The support plate is made of steel and, for this reason, it represents an important thermal mass capable of absorbing a large amount of heat. For simplicity, the simulation model has been assumed without taking into account the thermal constraints due to the weld clamping system (used in the experiments). This aspect could lead to notable differences in the cooling phase between the simulated curves and the measured curves in air-cooled joints. On the other hand, this difference is much less evident in water-cooled welds (Figure 5), where the useful time for transferring heat between the aluminium and

the steel plate is significantly reduced thanks to the presence of water which is able to quickly remove most of the heat developed by the process.

Figure 4 Simulated and measured values of temperature reached in air-cooled joint (see online version for colours)

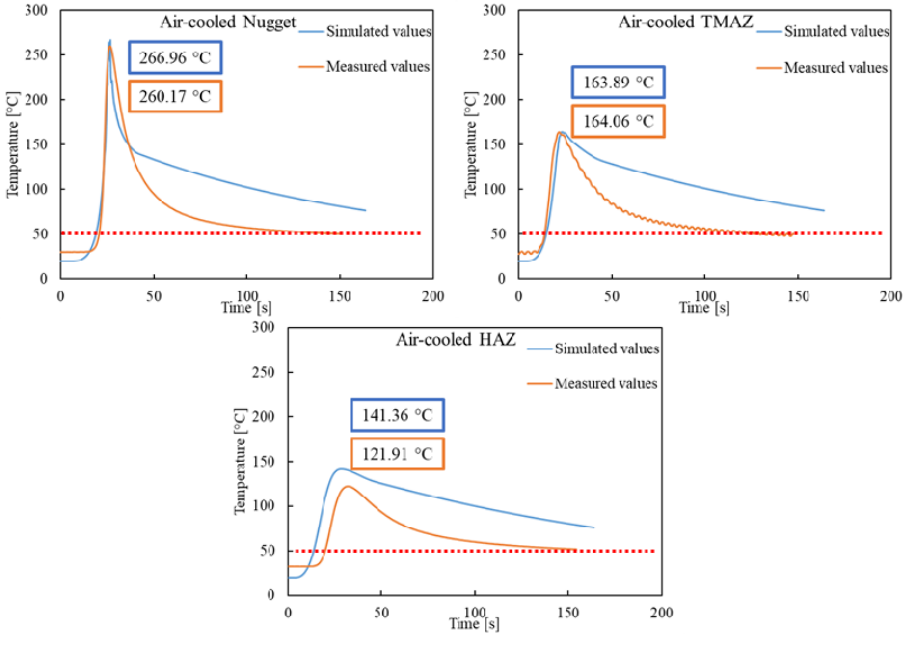

Figure 5 Simulated and measured values of temperature reached in water-cooled joints (see online version for colours)

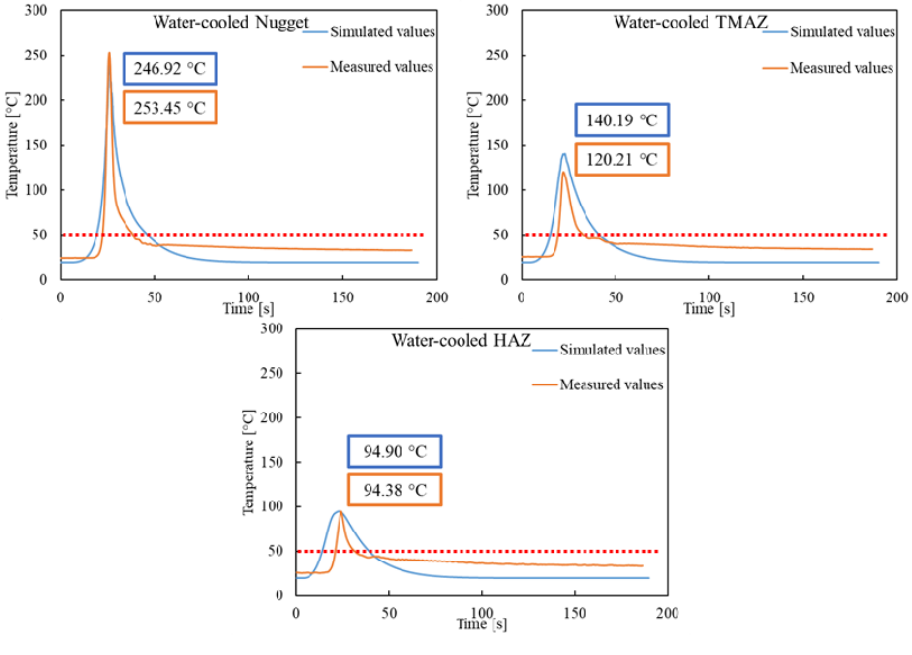

As far as the FEM model (Figure 6), following several experimental tests, the proposed model was calibrated. The model was successfully validated in different process conditions through the comparison with the corresponding experimental cases, thus demonstrating its robustness. Although the model was built using an AA6061, it is possible to assert that the validity of the thermal model is not linked to the use of a particular aluminium alloy, since there is no significant difference in thermal properties for 6000 and the other aluminium alloy series (Buffa et al., 2006).

Table 2 Considered combination of inputs and relating outputs for the air-cooled joints (see online version for colours)

Air-cooled joints							
	Input				*Output*		
	A	*B* (N/(mm·s·°C))	*C*	*D* (N/(mm·s·°C))	T_{nugget} (°C)	T_{TMAZ} (°C)	T_{HAZ} (°C)
#1	0.4	180.181	0.7	11	–52.40%	–44.40%	–40.20%
#2	0.4	180.181	0.7	110	–37.10%	–33.60%	–27.40%
#3	0.4	180.181	0.7	1100	–37.20%	–31.60%	–26.70%
#4	1.0	180.181	0.7	1100	–21.60%	–21.60%	–13.60%
#5	1.0	180.181	0.2	1100	–25.30%	–19.40%	–12.20%
#6	1.0	180.181	1	1100	–28.80%	–28.90%	–21.90%
#7	1.0	100.000	0.7	1100	–46.30%	–48.20%	–43.30%
#8	1.0	100.000	0.7	10000	–29.80%	–36.10%	–33.90%
#9	1.0	300.000	0.7	10000	–26.40%	–19.20%	–7.10%
#10	1.0	600.000	0.7	10000	–27.70%	–9.80%	9.10%
#11	1.0	450.000	0.7	10000	–19.60%	0.90%	17.60%
#12	0.4	100.000	0.2	8000	–10.90%	–42.90%	–41.70%
#13	1.0	450.000	0.7	10000	2.60%	–0.10%	15.90%

Table 3 Considered combination of inputs and relating outputs for the water-cooled joints (see online version for colours)

Water-cooled AA6082								
	INPUT					*OUTPUT*		
	A	*B* (N/(mm·s·°C))	*C*	*D* (N/(mm·s·°C))	E (N/(mm·s·°C))	T_{nugget} (°C)	T_{TMAZ} (°C)	T_{HAZ} (°C)
#1	1	450	0.7	10000	0.3	–7.90%	–15.20%	–3.70%
#2	1	450	0.7	10000	0.4	–4.30%	–9.10%	–2.10%
#3	1	450	0.7	10000	0.6	–8.60%	–23.90%	–15.80%

Figure 6 FEM model showing the temperature map for (a) air cooled and (b) water cooled process (see online version for colours)

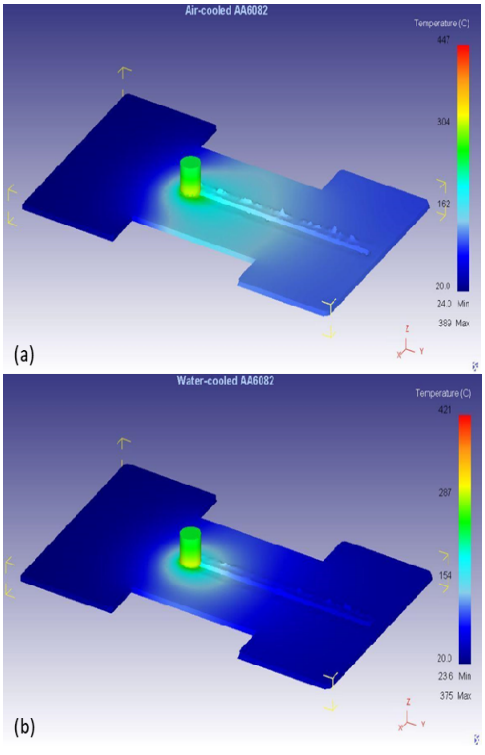

4 Implementation and validation of ANN

The neural network approach is one of the most powerful computer analysis techniques, based on the statistical regression, currently used in many fields of engineering for modelling complex relationships which are difficult to describe using physical models. The ANN utilised in the present study consists of three layers: input, hidden and output layers. The input layer information derived from the output of the FEM model. Specifically, temperature (T) and its acquisition point, in terms of X and Y positions, derived from the FEM simulation and the type of cooling applied (Cool) were taken into account. The process parameters have not been intentionally inserted among the inputs since the same welding speeds (feed rate and rotational speed) was used both for the experimental and the simulation part, as it is already optimised for this type of aluminium alloy.

The ANN aims to predict the value of hardness simply by knowing the temperature reached at a certain point during the welding process, since the reached temperature in the various areas plays a fundamental role, affecting the quantity of hardening precipitates present in the matrix, as it is demonstrated by Bocchi et al. (2021).

A single hidden layer was introduced, since the literature supports the idea of introducing few hidden layers to avoid an unnecessary complexity of the network. The number of hidden nodes (HN) is the most critical aspect for the neural network

architecture, since too few or too many nodes could generate an underfitting or overfitting. A trial and error approach was applied in a specific interval of nodes to determine the adequate dimension of hidden layer. The bounders of the hidden nodes interval hypothesis were defined through the most common heuristic technique found in literature. Specifically, the lower bound (equation (1)) is defined based on the theory developed by Garcia-Romeu et al. (2010); while the upper bound (equation (2)) was calculated based on the dimension of the training dataset according to the hypothesis and suggestion of Hagan et al. (2014).

$$MTI = \frac{IN + ON}{2} \tag{1}$$

$$N = \frac{R}{\alpha\left(IN + ON\right)} \tag{2}$$

where

- *MTI* is lower bound is heuristically defined by Her Majesty's Department of Trade and Industry
- *IN* is the number of input nodes.
- *ON* is the number of output nodes.
- *R* is the dimension of the training dataset.
- α is an arbitrary scaling factor usually 2–10. In this case, it was assumed $\alpha = 2$.

The trial and error procedure was performed through a Matlab code developed by the authors based on the scheme reported in Figure 7. Based on this procedure, a comparison between the provided output and the target values defined in the dataset is made for each HN hypothesis. Since the dataset contains a single output, for evaluating the prevision error between the imposed target and the predicted output, the Mean Square Error (MSE) was considered. Specifically, the hypothetical value of HN was fixed and the MSE was calculated; thus the configuration described by the lower value of MSE was selected as the optimal one.

The dataset was built based on the FEM and experimental results. Specifically, the temperature map was extracted from the FEM model indicating the temperature reached in several specific positions (x; y shown in Figure 8). The hardness was experimentally measured as a target of the training dataset for each combination. Rockwell B hardness tests (HRB) were performed following a 5-mm spaced grid in the central zone of the top of the specimen, according to ISO 6508.

The 70% of the entire dataset (318 cases) was used for the training activity, while the validation and tests stages exploited 15% each of the available data. As it is possible to observe from Figure 9, after the ANN training, the difference between the targets and the forecast outputs is very low and it is possible to observe that the defined ANN was properly trained. This means that the network will be able to predict, with an acceptable level of tolerance, the hardness of a specific area of the welded sheets, allowing to identify the mechanical characteristic and the main behaviour of the surface after the heat transfer due to the welding process.

Figure 7 ANN structure definition flowchart (see online version for colours)

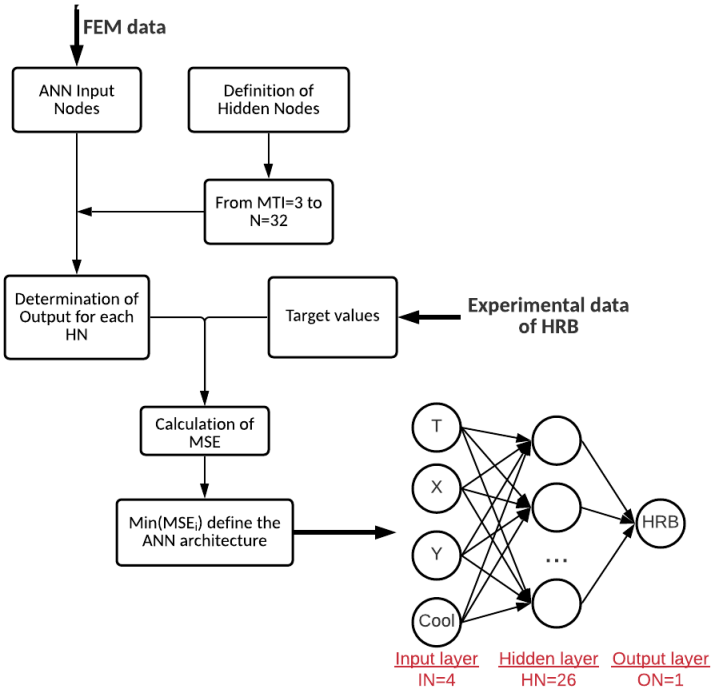

Figure 8 Reference system for identifying ordered pairs of points

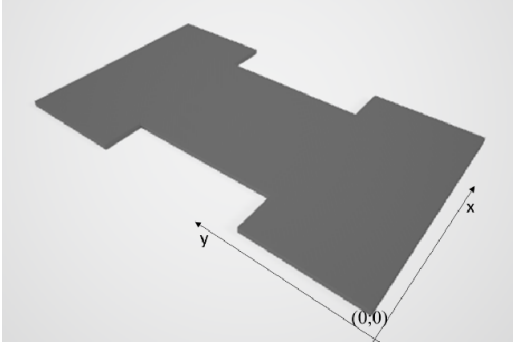

5 Results and discussion

The results obtained through the application of the developed FEM-ANN hybrid methodology fit very well the experimental data. The comparison between the experimental hardness curve and the curve of predicted hardness values obtained at $y = 45$ mm and $y = 135$ mm are shown in Figure 10 (air-cooled) and Figure 11 (water-cooled) as example. The graphs show how the typical W-shape of the FSWed junctions is maintained in the trend representation of the predicted values. The plots demonstrate the

reliability of the forecast data reporting a low deviation from the experimental results used for the validation. In fact, the general average error of prevision is approximately 3.65%.

Figure 9 ANN validation (see online version for colours)

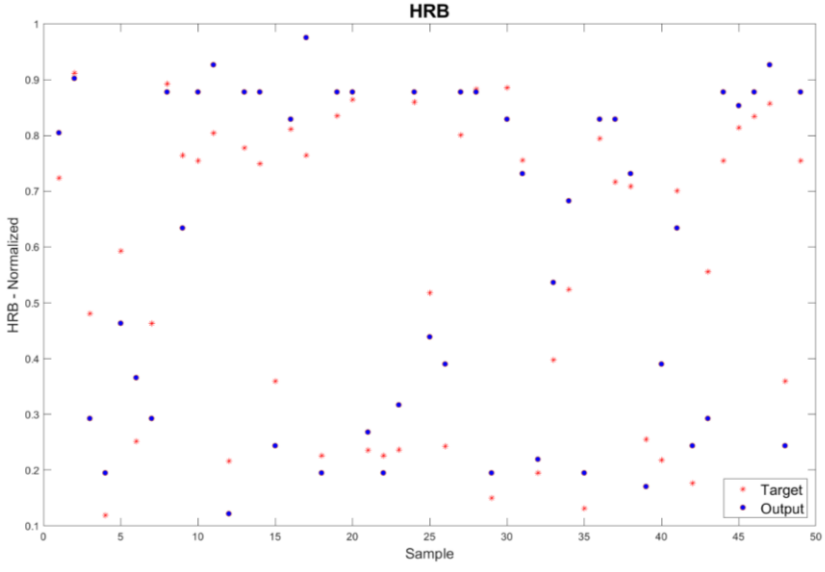

Figure 10 Application of hybrid FEM-ANN model to air-cooled FSW (see online version for colours)

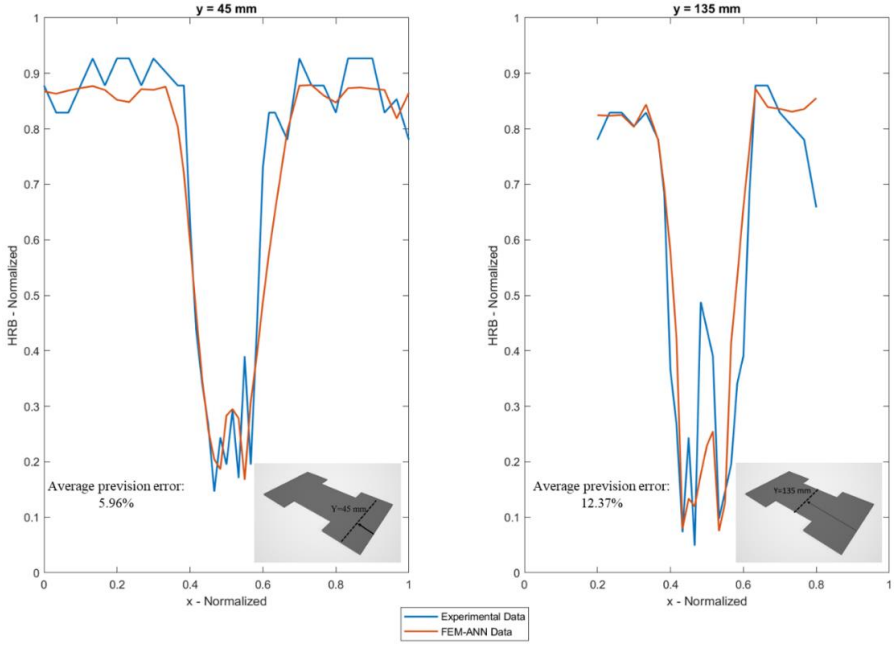

Figure 11 Application of hybrid FEM-ANN model to water-cooled FSW (see online version for colours)

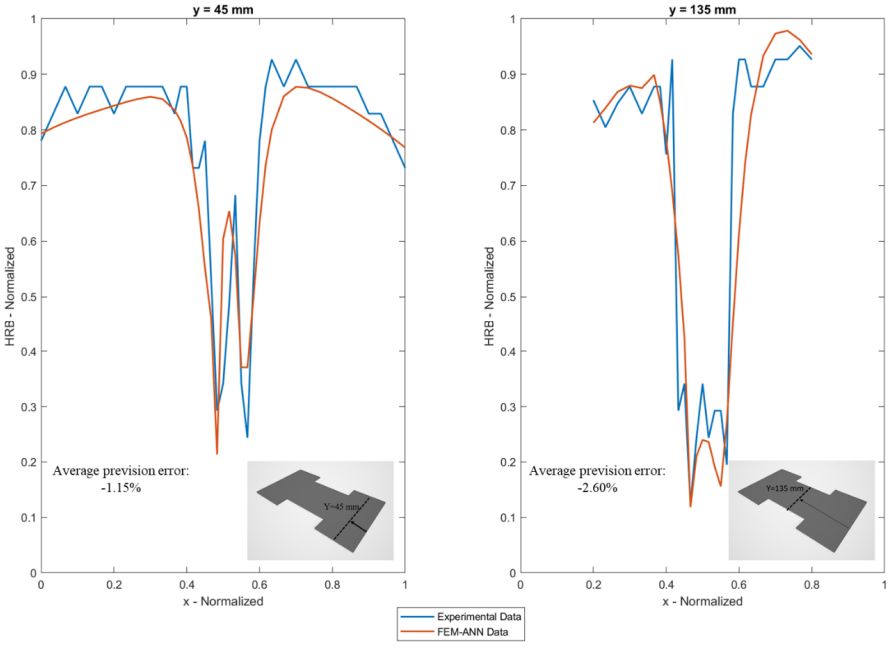

It is important to underline that to apply the proposed model, the developed hybrid approach must be capable of adequately predict the lower peak of hardness since it indicates the point where the break may occur. As can be observed in Figures 10 and 11, the model is able to approximate very well the minimum peak hardness values, identifying the typical points of failure of the FSW welds, mostly located near the interface between TMAZ and HAZ.

The need to research and investigate a relationship between the maximum temperature reached during the process and the final hardness corresponding to an exact point arises from the relation between the metallurgical phenomena occurring in the alloy and the mechanical behaviour of the joint. In particular, since AA6xxx is a precipitation hardening aluminium alloy, it is possible to state that the local mechanical characteristics of the piece, including therefore the hardness, are strongly linked to the microscopic state of the alloy structure, i.e., to the quantity and size of the hardening precipitates dispersed within the aluminium matrix.

These hardening precipitates, present in all precipitation hardening aluminium alloys, albeit formed by different alloying elements, give the alloy the highest level of mechanical behaviour only if present under specific conditions. The best hardening conditions occur only within a certain range of temperatures, characteristics for each alloy but well known and defined. These characteristic temperatures are linked to the presence of a transition temperature of the hardening precipitates above which the precipitates begin to coalescence and the matrix strengthening function is lost. Because of the described characteristic behaviour of precipitation hardening alloys, a systematic correlation between maximum temperatures and relative reached hardness was developed.

Finally, it is necessary to underline that the minimum hardness is reached at the interface between TMAZ and HAZ and not at the nugget, where the temperatures measured are the highest, because in the nugget the thermal effect of processing and the mechanical action of the pin coexist. The mechanical action of the pin acts on the material by mechanically breaking up the grains and hardening precipitates present in the matrix, thus ensuring a better mechanical response compared to the welding points where only the thermal contribution of the process acts without mixing the material.

6 Conclusions

The objective of this study was to develop a robust hybrid FEM-ANN approach that can be used for predicting the surface hardness in FSW for different cooling types starting from the peak of temperature reached during the welding process.

The Finite Element model set-up for the welding process cooled by air or water can supply a good prediction of the peak of temperature reached during the process on the entire surface of the samples. The neural network can exploit this information in order to have a quick prediction of the hardness of the specific point which is useful for identifying the mechanical characteristics of the part as a function of the area of interest. Specifically, it was shown how, once the hybrid approach was set-up and trained, the trends of predicted hardness fit very well with the corresponding experiments. In fact, it was possible to identify the different behaviour related to the different areas of the joint.

Finally, even if the developed hybrid FEM-ANN approach has been proposed for AA6082, it can be used for determining the final characteristics for welded joints of also all other precipitation hardening alloys, in order to forecasting the final characteristics and comparing them with the required data.

References

Arora, H.S., Singh, H. and Dhindaw, B.K. (2012) 'Numerical simulation of temperature distribution using finite difference equations and estimation of the grain size during friction stir processing', *Materials Science and Engineering A*, Vol. 543, pp.231–242.

Assidi, M., Fourment, L., Guerdoux, S. and Nelson, T.W. (2010) 'Friction model for friction stir welding process simulation: calibrations from welding experiments', *International Journal of Machine Tools and Manufacture*, Vol. 50, No. 2, pp.143–155.

Bevilacqua, M., Ciarapica, F.E., D'Orazio, A., Forcellese, A. and Simoncini, M. (2017) 'Sustainability analysis of friction stir welding of AA5754 sheets', *Procedia CIRP*, Elsevier, BV, pp.529–534.

Bocchi, S., D'Urso, G. and Giardini, C. (2021) 'The effect of heat generated on mechanical properties of friction stir welded aluminium alloys', *International Journal of Advanced Manufacturing Technology*, Vol. 112, Nos. 5–6, pp.1513–1528.

Bocchi, S., D'Urso, G., Giardini, C. and Maccarini, G. (2019) 'Effects of cooling conditions on microstructure and mechanical properties of friction stir welded butt joints of different aluminium alloys', *Applied Sciences*, Vol. 9, No. 23, p.5069.

Buffa, G., Hua, J., Shivpuri, R. and Fratini, L. (2006) 'A continuum based fem model for friction stir welding – model development', *Materials Science and Engineering A*, Vol. 419, Nos. 1–2, pp.389–396.

Chao, Y.J., Qi, X. and Tang, W. (2003) 'Heat transfer in friction stir welding–experimental and numerical studies', *Journal of Manufacturing Science and Engineering*, Vol. 125, No. 1, p.138.

Chen, C.M. and Kovacevic, R. (2003) 'Finite element modeling of friction stir welding – thermal and thermomechanical analysis', *International Journal of Machine Tools and Manufacture*, Vol. 43, No. 13, pp.1319–1326.

Colegrove, P.A., Shercliff, H.R. and Zettler, R. (2007) 'Model for predicting heat generation and temperature in friction stir welding from the material properties', *Science and Technology of Welding and Joining*, Vol. 12, No. 4, pp.284–297.

Dehabadi, V.M., Ghorbanpour, S. and Azimi, G. (2016) 'Application of artificial neural network to predict vickers microhardness of AA6061 friction stir welded sheets', *Journal of Central South University*, Vol. 23, No. 9, pp.2146–2155.

Fonda, R.W. and Bingert, J.F. (2004) 'Microstructural evolution in the heat-affected zone of a friction stir weld', *Metallurgical and Materials Transactions A: Physical Metallurgy and Materials Science*, Vol. 35A, No. 5, pp.1487–1499.

Garcia-Romeu, M.L., Ceretti, E., Fiorentino, A. and Giardini, C. (2010) 'Forming force prediction in two point incremental forming using backpropagation neural networks in combination with genetic algorithms', *ASME 2010 International Manufacturing Science and Engineering Conference, MSEC. 2010*, Pennsylvania, USA, pp.99–106.

Hagan, M.t., Demuth, H.B., Beale, M.H. and De Jesùs, O. (2014) *Neural Network Design*, 2nd ed., Neural Networks in a Softcomputing Framework.

He, X., Gu, F. and Ball, A. (2014) 'A review of numerical analysis of friction stir welding', *Progress in Materials Science*, pp.1–66.

Heirani, F., Abbasi, A. and Ardestani, M. (2017) 'Effects of processing parameters on microstructure and mechanical behaviours of underwater friction stir welding of Al5083 alloy', *Journal of Manufacturing Processes*, Vol. 25, pp.77–84.

IEA (2020) *Global Energy and CO*2 *Emissions in 2020 – Global Energy Review 2020 – Analysis – IEA*.

Lee, W.B., Yeon, Y.M. and Jung, S.B. (2004) 'Mechanical properties related to microstructural variation of 6061 al alloy joints by friction stir welding', *Materials Transactions*, Vol. 45, No. 5, pp.1700–1705.

Mishra, R.S. and Ma, Z.Y. (2005) 'Friction stir welding and processing', *Materials Science and Engineering R: Reports*, Vol. 50, Nos. 1–2, pp.1–78.

Qingzhao, W., Zhao, Z., Yong, Z., Yan, K. and Zhang, H. (2015) 'The adjustment strategy of welding parameters for spray formed 7055 aluminium alloy underwater friction stir welding joint', *Materials and Design*, Vol. 88, pp.1366–1376.

Ren, S.R., Ma, Z.Y. and Chen, L.Q. (2007) 'Effect of welding parameters on tensile properties and fracture behaviour of friction stir welded Al-Mg-Si alloy', *Scripta Materialia*, Vol. 56, No. 1, pp.69–72.

Rui-Dong, F., Zeng-Qiang, S., Rui-Cheng, S., Ying, L., Hui-Jie L. and Lei, L. (2011) 'Improvement of weld temperature distribution and mechanical properties of 7050 aluminium alloy butt joints by submerged friction stir welding', *Materials and Design*, Vol. 32, No. 10, pp.4825–4831.

Sethi, S.R., Das, A. and Baruah, M. (2021) 'A review on friction stir welding: a sustainable way of manufacturing', *Materials Today: Proceedings* [Preprint].

Shrivastava, A. and Krones, M., Pfefferkorn, F.E. (2015) 'Comparison of energy consumption and environmental impact of friction stir welding and gas metal arc welding for aluminium', *CIRP Journal of Manufacturing Science and Technology*, Vol. 9, pp.159–168.

Sönmez, F., Başak, H. and Baday, Ş. (2017) 'The mechanical strength of aluminium alloys which are joined with friction stir welding modelling with artificial neural networks', *IDAP.2017 - International Artificial Intelligence and Data Processing Symposium,* Institute of Electrical and Electronics Engineers Inc., pp.1–4.

Sorger, G., Wang, H., Vilaça, P. and Santos, T.G. (2017) 'FSW of aluminium AA5754 to steel DX54 with innovative overlap joint', *Welding in the World*, Vol. 61, No. 2, pp.257–268.

Wahid, M.A., Khan, Z.A. and Siddiquee, A.N. (2018) 'Review on underwater friction stir welding: a variant of friction stir welding with great potential of improving joint properties', *Transactions of Nonferrous Metals Society of China* (*English Edition*), Vol. 28, No. 2, pp.193–219.

Zhang, Z. and Zhang, H.W. (2008) 'A fully coupled thermo-mechanical model of friction stir welding', *International Journal of Advanced Manufacturing Technology*, Vol. 37, Nos. 3–4, pp.279–293.

Zhao, Y., Wang, Q., Chen, H. and Yan, K. (2014) 'Microstructure and mechanical properties of spray formed 7055 aluminium alloy by underwater friction stir welding', *Materials and Design*, Vol. 56, pp.725–730.

Zhu, X.K. and Chao, Y.J. (2004) 'Numerical simulation of transient temperature and residual stresses in friction stir welding of 304L stainless steel', *Journal of Materials Processing Technology*, Vol. 146, No. 2, pp.262–272.